

A game model for the multimodality phenomena of coauthorship networks

Zheng Xie^{1,‡}

1 College of Science, National University of Defense Technology, Changsha, China

‡ xiezheng81@nudt.edu.cn

Abstract

We provided a game model to simulate the evolution of coauthorship networks, a geometric hypergraph built on a circle. The model expresses kin selection and network reciprocity, two typically cooperative mechanisms, through a cooperation condition called positive benefit-minus-cost. The costs are modelled through space distances. The benefits are modelled through geometric zones that depend on node hyperdegree, which gives an expression of the cumulative advantage on the reputations of authors. Our findings indicate that the model gives a reasonable fitting to empirical coauthorship networks on their degree distribution, node clustering, and so on. It reveals two properties of node attractions, namely node heterogeneity and fading with the growth of hyperdegrees, can deduce the dichotomy of nodes' clustering behavior and assortativity, as well as the trichotomy of degree and hyperdegree distributions: generalized Poisson, power-law and exponential cutoff.

Introduction

Analyzing large-scale coauthorship data provides a macro-level view of collaboration patterns in scientific research, and has become an important topic of social sciences [1–4]. Coauthorship relationship can be expressed through a hypergraph, where nodes represent authors, and hyperedges express the author groups per paper. The simple graph extracted from the hypergraph is termed coauthorship network, where edges are generated by connecting each pair of the nodes belonging to the same hyperedge. Empirical coauthorship networks are featured by specific local (degree assortativity, high clustering) and global features (fat-tail, small-world) [5–10].

For general networks, these features have been reproduced by a range of important models, such as modeling fat-tail through preferential attachment or cumulative advantage [11–16], modeling degree

assortativity by connecting two non-connected nodes that have similar degrees [17]. For coauthorship networks, can these emerged features be deduced through cooperative mechanisms? The five typical mechanisms of cooperations exist in the evolution of coauthorship networks [18]. Coauthoring behavior often occurs in a research group (kin selection). Cooperation contributes to achieve breakthroughs and reputations (direct and indirect reciprocity). Sociable researchers and famous research teams are easy to attract collaborators (network reciprocity, group selection).

The inhomogeneity of node influences is an alternative explanation for fat-tail [19]. Nodes with wider influences are likely to gain more connections. The idea has been adopted to simulate the evolution of coauthorship networks, in which node influences are modelled by attaching specific geometric zones to nodes [20, 21]. The corresponding models, geometric hypergraphs, provide reasonable model-data fittings. The work in Ref. [10] gives an explanation for the models' mechanism from the perspective of cooperative game. The costs are modelled through space distances, and the benefits are expressed through node reputations. Node reputations cumulate over time. The cooperation condition is positive benefit-minus-cost.

We provided a game model for coauthorship networks based on the cumulative advantage on reputations: supposing reputation to be a function of node hyperdegree (a node's hyperdegree is the number of the hyperedges containing the node). The function has a flexibility to reproduce the trichotomy of degree and hyperdegree distributions, namely a generalized Poisson head, a power-law in the middle part, and an exponential tail. In addition, nodes' clustering behavior and assortative behavior are different from small degree nodes to large degree nodes. These dichotomous phenomena are also predicted by the model.

This paper is organized as follows: The model and data are described in Section 2 and 3 respectively; the multimodality phenomena are discussed in Section 4 and 5; Conclusions are drawn in Section 6.

The model

A cooperative game consists a set of players and a characteristic function specifying the value (benefit-minus-cost) created by subsets of players in the game. Coauthorship networks can be regarded as the results of such a game. Researchers can be viewed as players. Coauthoring a researcher with high reputation is a kind of benefits, contributing to academic success. The investments of manpower and

material resources on research are the costs of cooperations. We presented an implement of the game of coauthoring behavior through a geometric hypergraph, expressing the reputations and costs through a function of hyperdegree and that of geometric distance respectively.

The model is built on a circle S^1 as follows. Sprinkle a set of nodes N_t on S^1 uniformly and randomly at each time $t \in [1, T]$, where $T \in \mathbb{Z}^+$. Select a subset N_t^l from N_t randomly as lead nodes. Each lead node i is assigned an arc with centre θ_i to imitate its reputation. The length of the arc is

$$r_i(t) = \frac{\alpha}{t} (h_i(t) + 1)^{e^{-\beta(k_i(t)+1)}}, \quad (1)$$

where $h_i(t)$ is the hyperdegree of node i at time t , α and $\beta \in \mathbb{R}^+$. The group of the nodes covered by a lead node's arc expresses a research team.

Coauthoring behavior is expressed through hyperedges generated as follows. For each new node $j(\theta_j, t_j) \in N_t$, select a lead node set M_j^l for which $\forall i(\theta_i, t_i) \in M_j^l$ satisfies $r(i) > \pi - |\pi - |\theta_i - \theta_j||$ and $t_i < t_j$. It means node j 's reputation is larger than the angular distance between i and j , an expression of positive benefit-minus-cost. For each $i \in M_j^l$, we append j to R_i (a set used to model node i 's research team), and generate a hyperedge at probability p by grouping i, j , $(\min(x, |R_i|) - 2)$ nodes of R_i nearest to j , and $(x - \min(x, |R_i|))$ nodes $\notin R_i$ randomly, where x is the random variable of an inputting distribution, a fitting of the empirical distributions of hyperedge sizes.

The way of generating hyperedges describes a usual scene of cooperation. A researcher wants to complete a work, which needs several researchers to work together. Then he would ask his team leader for help. The leader would suggest some team members with similar interest to work together. Such behavior can be viewed as kin selection. When finishing the work is beyond the ability of the team, the researcher would ask for external helpers. This inspires the design of randomly choosing $(x - \min(x, |R_j|))$ nodes outside of R_j to cooperate.

The random variable x , used to model hyperedge size, is generated as follows. Give the upper bound of small research team $\mu > 0$, and the lower bound of large research team $\nu > 0$. Denote the expected value of hyperedge sizes and the size of R_i to be η and λ . Let $\eta = \min\{\lambda, \mu\}$ if $\lambda \leq \nu$, and draw η from a power law distribution with an exponent γ and domain $[\mu, \lambda]$ if $\lambda > \nu$. Draw x from a Poisson distribution with the expected value η .

We assumed each lead node has the same attraction to new nodes, and so let the reputation of a

lead node $i(\theta_i, t_i)$ be $r(i) \propto 1/t_i$ (which is inherited from the PSO model [22]). The novel aspect we introduced is the fading heterogeneity over hyperdegrees. When a node’s zonal size fades to a value free of its hyperdegree, the probability of receiving connections is the same as that of the standard random graph, which has an exponentially decaying hyperdegree distribution. In contrast, if its hyperdegree is not large enough, then cumulative advantage is significant, which gives rise to the power law part of hyperdegree distributions.

Compared with the model in Ref. [21], our model removes the hypothesis of the arc-length being a power function of nodes’ birth time, thus gives a direct simulation of the cumulative advantage for hyperdegrees and degrees. It expresses a typically cooperative mechanism, namely network reciprocity. In addition, compared with that previous model, our model has the ability to predict the transition from power law to exponential cutoff for hyperdegree and degree distributions, thus fully reproduces the trichotomy of these distributions.

The data

We analyzed two empirical coauthorship datasets collected from Web of Science (www.webofscience.com). Dataset PNAS is composed of 36,732 papers published in *Proceedings of the National Academy of Sciences* during 2007–2015. Dataset PRE comprises 24,079 papers published in *Physical Review E* during 2007–2016. The different collaboration level (reflected by the average number of the authors per paper) of the two datasets (PNAS 6.712, PRE 3.102) helps to test model flexibility.

The entities of persons are identified by authors’ name on their papers, which constitute the nodes of the empirical networks analyzed here. Table 1 shows certain statistical indexes for these networks. Note that these networks suffer errors: one person is identified as two or more entities (splitting error); two or more persons are identified as one entity (merging error). The analysis in Appendix A shows the multimodality phenomena considered here are robust to these errors at certain levels.

We modelled two hypergraphs to reproduce the multimodality phenomena emerged in the empirical networks. The reason of choosing their parameters (Table 2) is as follow. We valued μ through the expected value of the general Poisson part of an empirical distribution of hyperedge sizes (Fig. 1), and valued ν through iteration from the starting point of the power-law part of the distribution until the distribution of modelled hyperedge sizes is similar to the empirical one. We valued α , $|N_t|$, $|N_t^l|$ and p to

Table 1. Specific statistical indexes of empirical networks.

Network	NN	NE	GCC	AC	AP	PG
PNAS	161,780	1,074,836	0.896	0.554	6.599	0.848
PRE	37,528	90,711	0.838	0.394	6.060	0.583
PNAS-s	115,462	1,049,253	0.832	0.064	4.176	0.968
PRE-s	27,925	86,648	0.773	0.237	6.148	0.814
Synthetic-1	103,816	613,466	0.574	0.255	12.23	0.574
Synthetic-2	34511	73665	0.826	0.338	13.63	0.440

The indexes are the numbers of nodes (NN) and edges (NE), global clustering coefficient (GCC), assortativity coefficient (AC), the average shortest path length (AP), and the node proportion of the giant component (PG). The values of AP of the first, third and fifth networks are calculated by sampling 300,000 pairs of nodes. The networks with suffix -s are used in Appendix A.

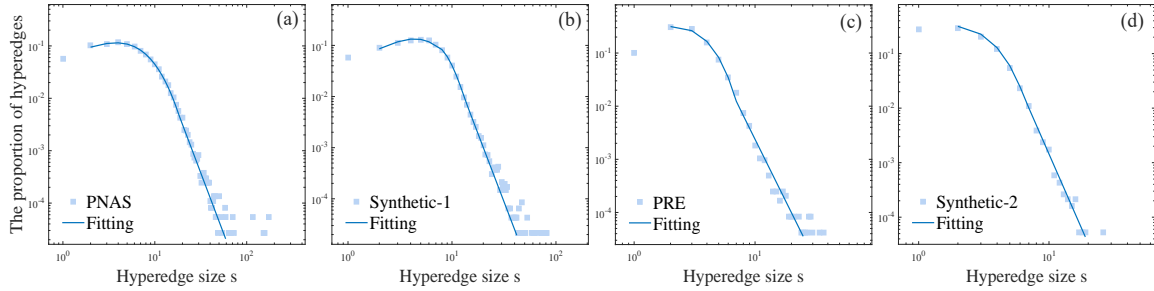


Figure 1. The distributions of hyperedge sizes. Each fitting is a mixture of a generalized Poisson and a power-law distribution. The fitting process and goodness-of-fit are shown in Appendix B.

make the hyperdegrees of substantial nodes be one.

Table 2. The parameters of synthetic networks.

$T = 6, 000, 9, 000$	$N_t = 100, 15$	$N_t^l = 5, 5$	$p = 0.25, 0.4$
$\alpha = 0.073, 0.19$	$\gamma = 0.001, 0.00001$	$\mu = 6, 2$	$\nu = 42, 6$

The parameters in the first row control network size, and those in the second row control the distribution of hyperedge sizes, degree and hyperdegree distribution.

The trichotomous distributions of degrees and hyperdegrees

The trichotomy of degree and hyperdegree distributions comprises a generalized Poisson head, a power-law in the middle part, and an exponential tail (Fig. 2). The power law parts are fitted through the method of Clauset et al [23]. The generalized Poisson distributions and the power law functions with an exponential cutoff are fitted through maximum-likelihood estimation. The fitting process and goodness-

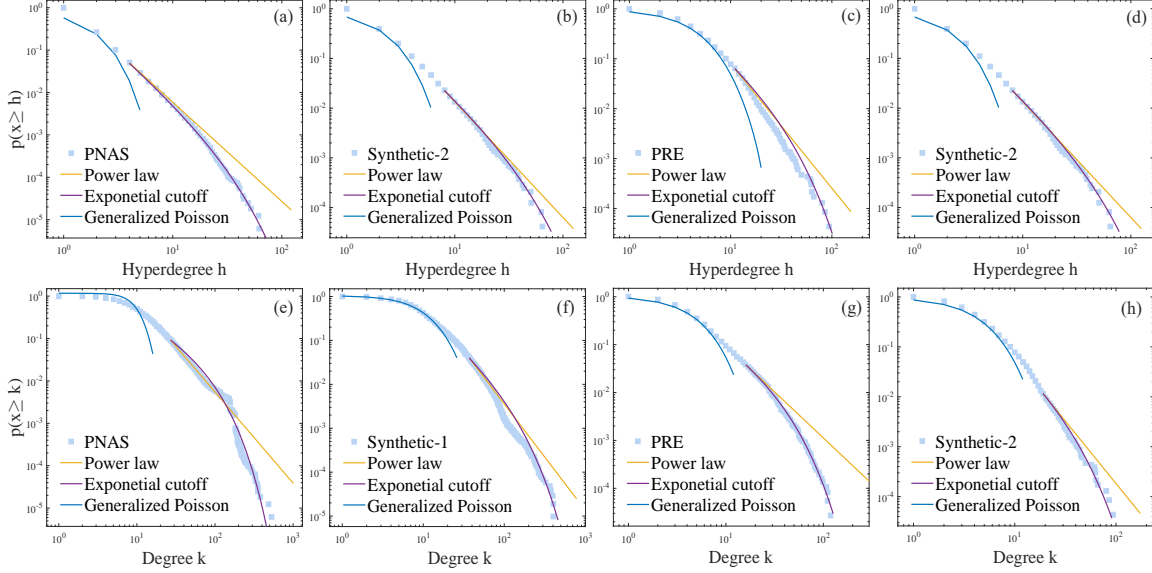


Figure 2. The cumulative distributions of hyperdegrees and degrees. Panels show these cumulative distributions of the empirical and synthetic datasets, as well as their trichotomy.

of-fit are shown in Appendix C.

Generalized Poisson distributions can be derived from a range of “coin flipping” behaviors, where the probability of observing “head” is dependent on observed events [24]. The event of publishing a paper is kind of observing “head” (reject or accept), where the probability of publishing is also affected by previous events. For example, an author would easily write his second paper, compared with his first one. There is a cumulative advantage in writing papers, writing experiments accumulating in the process of publishing papers. In hyperdegree distributions, the process reflects as the transition from generated Poisson distribution to power law. Meanwhile, aging is against cumulative advantage, which reflects as the transition from power law to exponential cutoff.

Fig. 2 shows our model can fully reproduce the trichotomy. The modelled hyperedges are generated through an inhomogeneous Poisson point process (namely its density of points is not a constant), because the probability of new nodes fallen in a lead node’s zone depends on the lead node’s hyperdegree. At each time t , the expected number of new hyperedges $r_i(t)m/2\pi$ is a function of $h_i(t)$, the real-time hyperdegree at time t . Therefore, the hyperdegree $h_i(T)$ follows a generalized Poisson distribution. When $h_i(T)$ is

sufficiently large and $\beta(h_i(t) + 1) \ll 1$, the formula (1) gives rise to

$$\frac{d}{dt}h_i(t) = \frac{m}{2\pi}r_i(t) \approx \frac{\lambda}{t}(h_i(t) + 1), \quad (2)$$

where $\lambda = \alpha m/2\pi$. The solution to Eq. (2) gives node i 's expected hyperdegree $\bar{h}_i(T) = (T/t_i)^\lambda - 1$, which gives rise to $p(\bar{h}_i(T) \leq h) = p(t_i \geq T/(h+1)^{1/\lambda})$. Based on the mean-field theory, we deduced its density function as follows. The probability of a node generated at t_i is $1/T$. Hence $p(t_i \geq T(h+1)^{-1/\lambda}) = 1 - p(t_i < T(h+1)^{-1/\lambda}) = 1 - (h+1)^{-1/\lambda}$, which gives rise to a power-law distribution

$$p(h) = \frac{d}{dh}p(\bar{h}_i(T) \leq h) \propto (h+1)^{-1-\frac{1}{\lambda}} \approx h^{-1-\frac{1}{\lambda}} \quad (3)$$

for sufficiently large h . It shows the transition from generalized Poisson distribution to power law.

When $\beta(h_i(t) + 1) \gg 1$, the formula (1) gives rise to

$$\frac{d}{dt}h_i(t) = \frac{m}{2\pi}r_i(t) \approx \frac{\lambda}{t}. \quad (4)$$

The solution to Eq. (4) gives node i 's expected hyperdegree $\bar{h}_i(T) = \lambda \log(T/t_i) + \delta$, where δ is the hyperdegree accumulated from the process governed by Eq. (2). It yields $p(\bar{h}_i(T) \leq h) = p(t_i \geq Te^{-(h-\delta)/\lambda})$. Hence $p(t_i \geq Te^{-(h-\delta)/\lambda}) = 1 - p(t_i < Te^{-(h-\delta)/\lambda}) = 1 - e^{-(h-\delta)/\lambda}$. It gives rise to

$$p(h) = \frac{d}{dh}p(\bar{h}_i(T) \leq h) \propto \frac{1}{\lambda}e^{-\frac{h-\delta}{\lambda}}, \quad (5)$$

which is an exponential distribution on the interval $[\delta, +\infty)$. Therefore, we can expect a power law with an exponential cutoff for sufficiently large hyperdegrees, namely $p(h) \propto h^{-1-1/\lambda}e^{-h/\lambda}$.

Now we turn to the trichotomy of degree distributions (Fig. 2). The hyperdegrees of many nodes are equal to one (PNAS: 74.0%, PRE: 63.9%). As Fig. 1 shows, most of hyperedge sizes follow a generated Poisson distribution (PNAS: 99.9%, PRE: 99.9%). Those lead the generalized Poisson parts of degree distributions. Meanwhile, nodes' hyperdegree positively correlates to their degree (Fig. 3), the growing process of hyperdegrees coupling with that of degrees. The positive correlation leads the multimodality of degree distributions. Note that the nodes of hyperedges with a large size also have a large degree, which leads the outliers in the tails of degree distributions.

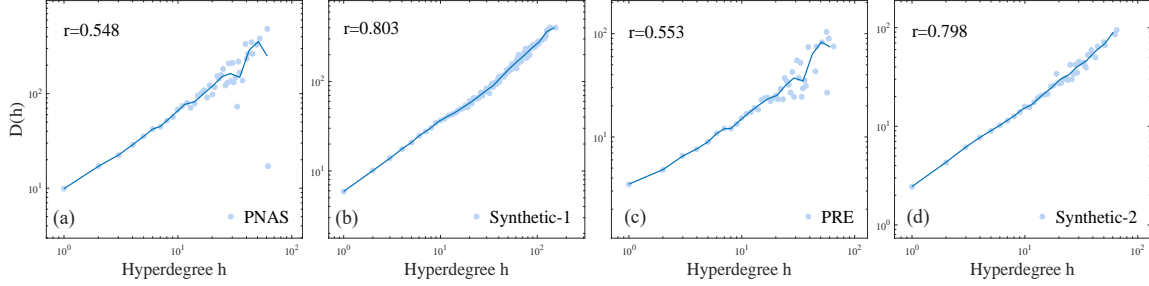


Figure 3. The positive correlation between degrees and hyperdegrees. Function $D(h)$ is the average degree of the nodes with hyperdegree h . Index r is the Pearson’s linear correlation coefficient. Data are binned on abscissa axes to improve visibility for the positive slopes.

In synthetic data, The hyperdegrees of a large fraction of nodes are equal to one (Synthetic-1: 47.0%, Synthetic-2: 60.7%). The sizes of most modelled hyperedges follow a generalized Poisson distribution (Synthetic-1: 99.8%, Synthetic-2: 99.7%). Those yield the generalized Poisson part of modelled degree distributions. Meanwhile, the model preserves the positive correlation between hyperdegrees and degrees, especially $h(t) \propto k(t)$ for the nodes with a large hyperdegree. Therefore, it can reproduce the multimodality of degree distributions.

The dichotomous phenomenon in clustering and assortativity

Coauthorship networks are found to have two features: high clustering (a high probability of a node’s two neighbors connecting) and degree assortativity (nodes’ degree positively correlates to their average degree of neighbors), which are reflected through the high values of their global clustering coefficient and assortative coefficient (Table 1).

Observing these features over degrees, we can find that they differ from small degree nodes to large degree nodes. Consider the average local clustering coefficient of k -degree nodes $C(k)$ and the average degree of k -degree nodes’ neighbors $N(k)$. We can find the dichotomy of the functions $C(k)$ and $N(k)$ (Fig. 4).

The dichotomy is due to the positive correlation between hyperdegrees and degrees. A large fraction of nodes with a small degree only belong to a few hyperedges. Their neighbors probably connect to each other, and only a few of their neighbors have a large degree. Therefore, over small k , the value of $C(k)$ is high, and the slope of $N(k)$ is positive. Consider the small fraction of nodes with a large degree.

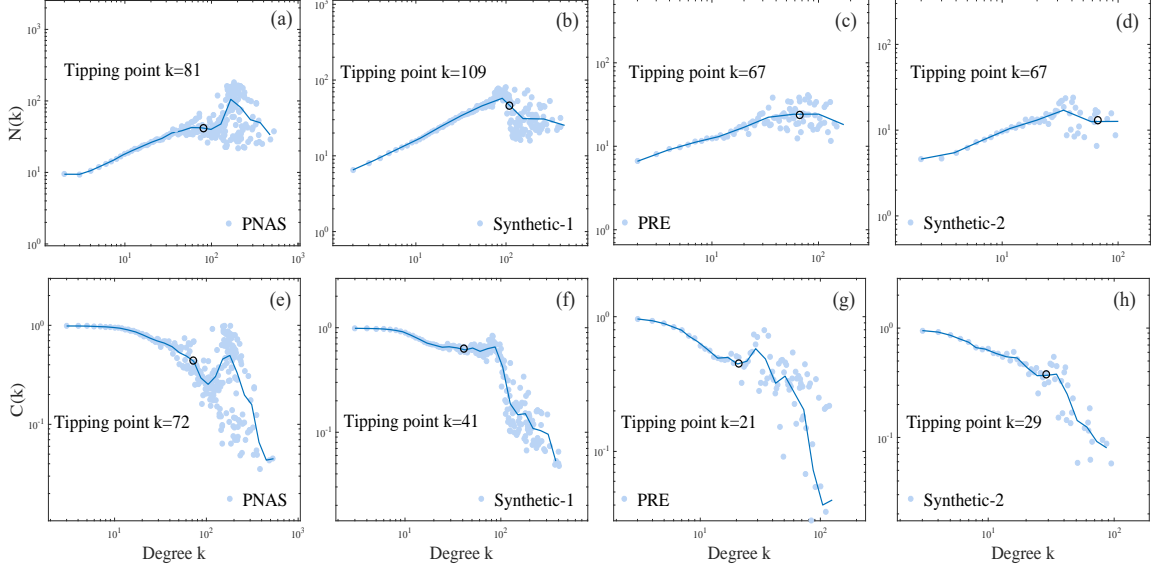


Figure 4. The average local clustering coefficient of k -degree nodes $C(k)$ and the average degree of k -degree nodes' neighbors $N(k)$. The tipping points of the two functions are detected by the boundary point detection algorithm for general functions in Ref. [21], which is listed in Appendix C.

These nodes probably have a large hyperdegree. Their neighbors in different hyperedges probably do not connect with each other and have a small degree. Otherwise, there will be many nodes with a large degree, out of touch with reality. Therefore, the slopes of $C(k)$ and $N(k)$ over large k are negative. Our model captures the positive correlation, thus gives a reasonable fit to the dichotomy.

Discussion and conclusions

A hypergraph model is provided to simulate the evolution of coauthorship networks from the perspective of cooperative game, which expresses two cooperative mechanisms, kin selection and network reciprocity, in a geometric way. It predicts a range of features of coauthorship networks, such as fat-tail, small-world, etc. Especially, it reproduces the trichotomous distributions for degrees and hyperdegrees, as well as the dichotomous phenomena in clustering and assortativity. It overcomes the weakness of the model in Ref. [20], providing a direct simulation of the cumulative advantage on writing experiments.

The model provides an example of how individual strategies based on positive benefit-minus-cost and on specific randomness generate the complexity emerged in coauthorship networks. It can be extended to analyze the coevolution with citation behavior [25]. It also has the potential to be a null model in the

empirical analysis of social affiliation networks. Whereas other typically cooperative mechanisms should be addressed, such as group selection, direct and indirect reciprocity.

Acknowledgments

This work is supported by National Science Foundation of China (Grant No. 61773020).

References

1. Glänzel W, Schubert A (2004) Analysing scientific networks through co-authorship. *Handbook of quantitative science and technology research* 11: 257-276.
2. Glänzel W (2014) Analysis of co-authorship patterns at the individual level. *Transinformacao* 26: 229-238.
3. Sarigöl E, Pfitzner R, Scholtes I, Garas A, Schweitzer F (2014) Predicting scientific success based on coauthorship networks. *EPJ Data Science* 3(1): 1-16.
4. Mali F, Kronegger L, Doreian P, Ferligoj A, Dynamic scientific coauthorship networks (2012) In: Scharnhorst A, Börner K, Besselaar PVD editors. *Models of science dynamics*. Springer. pp. 195-232.
5. Newman M (2001) Scientific collaboration networks. I. network construction and fundamental results. *Phys Rev E* 64: 016131.
6. Newman M (2001) Scientific collaboration networks. II. shortest paths, weighted networks, and centrality. *Phys Rev E* 64: 016132.
7. Newman M (2001) The structure of scientific collaboration networks. *Proc Natl Acad Sci USA* 98: 404-409.
8. Newman M (2004) Coauthorship networks and patterns of scientific collaboration. *Proc Natl Acad Sci USA* 101: 5200-5205.
9. Newman M (2002) Assortative mixing in networks. *Phys Rev Lett* 89: 208701.

10. Xie Z, Li M, Li JP, Duan XJ, Ouyang ZZ (2018) Feature analysis of multidisciplinary scientific collaboration patterns based on pnas. *EPJ Data Science* 7: 5.
11. Barabási AL, Jeong H, Neda Z, Ravasz E, Schubert A, Vicsek T. (2002) Evolution of the social network of scientific collaborations. *Physica A* 311: 590-614.
12. Moody J (2004) The structure of a social science collaboration network: disciplinary cohesion from 1963 to 1999. *Am Sociol Rev* 69(2): 213-238.
13. Perc C (2010) Growth and structure of Slovenia's scientific collaboration network. *J Informetr* 4: 475-482.
14. Wagner CS, Leydesdorff L (2005) Network structure, self-organization, and the growth of international collaboration in science. *Res Policy* 34(10): 1608-1618.
15. Tomassini M, Luthi L (2007) Empirical analysis of the evolution of a scientific collaboration network. *Physica A* 285: 750-764.
16. Santos FC, Pacheco JM (2005) Scale-free networks provide a unifying framework for the emergence of cooperation. *Phys Rev Lett* 95(9): 098104.
17. Catanzaro M, Caldarelli G, Pietronero L (2004) Assortative model for social networks. *Phys Rev E* 70: 037101.
18. Nowak MA (2006) Five rules for the evolution of cooperation. *Science* 314(5805): 1560-3.
19. Krioukov D, Kitsak M, Sinkovits RS, Rideout D, Meyer D, Boguñá M (2012) Network cosmology. *Sci Rep* 2: 793.
20. Xie Z, Ouyang ZZ, Li JP (2016) A geometric graph model for coauthorship networks. *J Informetr* 10: 299-311.
21. Xie Z, Ouyang ZZ, Li JP, Dong EM, Yi DY (2018) Modelling transition phenomena of scientific coauthorship networks. *J Assoc Inf Sci Technol* 69(2): 305-317.
22. Papadopoulos F, Kitsak M, Serrano MA, Boguñá M, Krioukov D (2012) Popularity versus similarity in growing networks. *Nature* 489: 537-540.

23. Clauset A, Shalizi CR, Newman MEJ (2009) Power-law distributions in empirical data. *SIAM Rev* 51: 661-703.
24. Consul PC, Jain GC (1973) A generalization of the Poisson distribution. *Technometrics* 15(4): 791-799.
25. Xie Z, Xie ZL, Li M, Li JP, Yi DY (2017) Modeling the coevolution between citations and coauthorship of scientific papers. *Scientometrics* 112: 483-507.
26. Milojević S (2010) Modes of collaboration in modern science-beyond power laws and preferential attachment. *J Assoc Inf Sci Technol* 61(7): 1410-1423.
27. Kim J, Diesner J (2016) Distortive effects of initial-based name disambiguation on measurements of large-scale coauthorship networks. *J Assoc Inf Sci Technol* 67(6): 1446-1461.

Appendix A

Ambiguities exist in coauthorship data, known as merging and splitting errors. Since there are many nodes with a small degree or hyperdegree, these errors do not change the feature of the heads of degree and hyperdegree distributions, as well as the heads of $C(k)$ and $N(k)$. Merging errors can ruin the exponential cutoff, because they generate nodes with a degree far more than ground truth. Splitting errors generate nodes with a degree smaller than ground truth, thus would generate exponential cutoff.

Consider a network suffering heavy merging errors and free of splitting errors. If the network has an exponential cutoff in its degree and hyperdegree distribution, we could say these distributions of the corresponding ground-truth network has an exponential cutoff. In fact, the density function of the summation of two random variables drawn from an exponential distribution still has an exponential factor. Generate entities through short name (surname and the initial of the first given name) and use them to construct networks (PNAS-s, PRE-s). These networks are almost free of splitting errors (unless an author provides a wrong name), but heavily suffer merging errors. Table 1 shows certain statistical indexes of these networks. Fig. 5 shows the degree and hyperdegree distribution still have an exponential cutoff, which means the cutoff exists in the corresponding ground-truth distributions.

Merging errors satisfying specific distribution can generate a power law. Therefore, our conclusions are drawn under the assumption that the ground-truth coauthorship networks have a power law part in

their degree and hyperdegree distribution, because the considered data are not free merging errors. The explanation for the features of the tails of $C(k)$ and $N(k)$ is also dependent on this assumption.

To show the reasonability of this assumption, we computed the proportion of short names in the names on papers, and that of the short names appearing in more than one paper, because using short names will generate a lot of merging errors [26]. Chinese names were also found to account for merging errors [27]. For the names on papers, we counted the proportion of the names consisting of a surname among major 100 Chinese surnames and a given name less than six characters. The small proportions of such names and those of such names appearing in more than one paper imply the impacts of merging errors are limited, especially for the dataset PNAS (Table 4).

Table 3. Specific statistical indexes of the empirical data.

Data	a	b	c	d
PNAS	1.40%	0.13%	3.11%	1.30%
PRE	19.2%	6.45%	3.85%	1.58%

Indexes a and b are the proportion of short names in the names on papers, and the proportion of the short names appearing in more than one paper. Indexes c and d are the proportion of the names consisting of a surname among major 100 Chinese surnames and only one given name shorter than six characters, and the proportion of such names appearing in more than one paper.

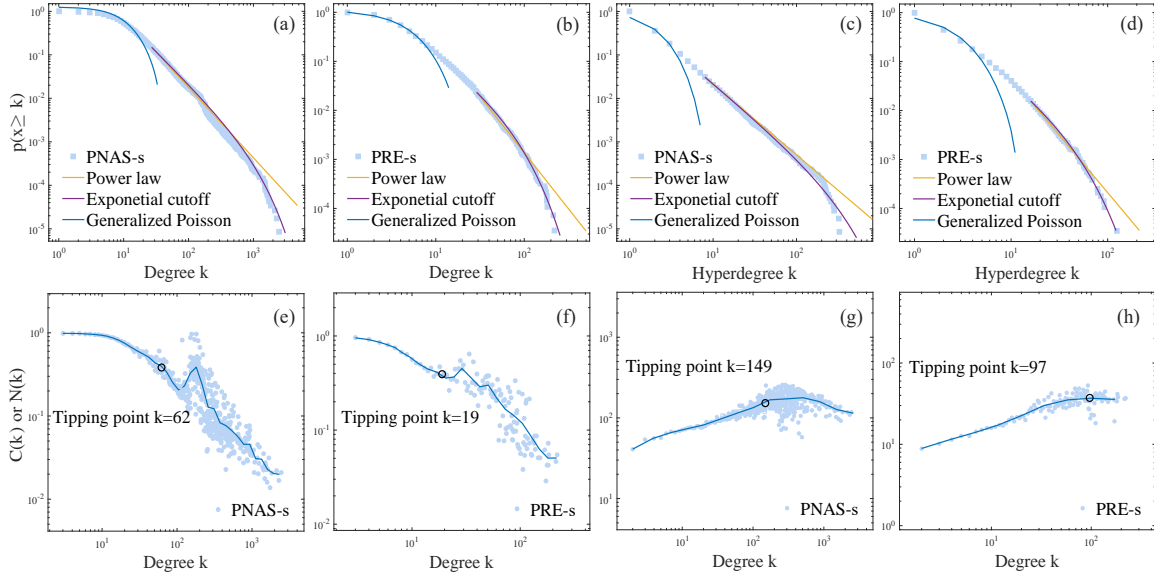


Figure 5. The multimodality phenomena of the networks generated by using short names. Panels show these networks' degree and hyperdegree distribution, $C(k)$ and $N(k)$.

Appendix B

The empirical distribution of hyperedge sizes can be fitted by a mixture of a generalized Poisson distribution and a power law. Let the domains of generalized Poisson $f_1(x) = a(a + bx)^{x-1}e^{-a-bx}/x!$, cross-over and power-law $f_2(x) = cx^{-d}$ be $[\min(x), E]$, $[B, E]$ and $[B, \max(x)]$ respectively. The fitting function defined on $[\min(x), \max(x)]$ is $f(x) = q(x)sf_1(x) + (1 - q(x))f_2(x)$, where $q(x) = e^{-(x-B)/(E-x)}$. The fitting processes are: calculate parameters of $sf_1(x)$ and $f_2(x)$ by regressing the head and tail of empirical distribution respectively; find B and E through exhaustion to make $f(x)$ pass the Kolmogorov-Smirnov (KS) test ($p\text{-value} > 0.05$). The fitting results are listed in Table 4.

Table 4. The fitting of the distribution of hyperedge sizes.

Networks	a	b	c	d	s	B	E	$p\text{-value}$
PNAS	3.504	0.444	2,086	4.428	1.159	12	32	0.913
Synthetic-1	4.406	0.234	1,919	4.794	1.056	7	18	0.074
PRE	2.507	0.000	92.00	4.587	1.249	6	7	0.133
Synthetic-2	2.067	0.049	409.9	5.454	1.156	5	6	0.651

The p -value of KS test is a measurement of goodness-of-fit.

Appendix C

Table 5 shows the boundary detection algorithm for generalized Poisson distributions. The observations $\{D_s, s = 1, \dots, n\}$ are nodes' degree or hyperdegree. Changing the algorithm as follows, we can obtain the boundary of the power law functions with an exponential cutoff. For k from 1 to $\max(D_1, \dots, D_n)$, we fit $h(\cdot)$ to the density $h_0(\cdot)$ of $\{D_s, s = 1, \dots, n | D_s \geq k\}$, until the KS test accepts the null hypothesis.

Table 6 shows the corresponding goodness-of-fit.

Table 7 shows the boundary detection algorithm for the average local clustering coefficient of k -degree nodes $C(k)$ and the average degree of k -degree nodes' neighbors $N(k)$. The inputs are $g(\cdot) = \log(\cdot)$, $h(s) = a_1e^{-((s-a_2)/a_3)^2}$ for $C(k)$, and $h(s) = a_1s^3 + a_2s^2 + a_3s + a_4$ for $N(k)$, where $s, a_i \in \mathbb{R}$ ($i = 1, \dots, 4$). Using these inputs is based on the observations on $C(k)$ and $N(k)$.

Table 5. A boundary detection algorithm of generalized Poisson distributions [21].

Input: Observations $D_s, s = 1, \dots, n$, rescaling function $g(\cdot)$, and fitting model $h(\cdot)$.

For k from 1 to $\max(D_1, \dots, D_n)$ do:
 Fit $h(\cdot)$ to the PDF $h_0(\cdot)$ of $\{D_s, s = 1, \dots, n | D_s \leq k\}$ by maximum-likelihood estimation;
 Do KS test for two data $g(h(t))$ and $g(h_0(t)), t = 1, \dots, k$ with the null hypothesis they coming from the same continuous distribution;
 Break if the test rejects the null hypothesis at significance level 5%.

Output: The current k as the boundary point.

Table 6. The goodness-of-fit of degree and hyperdegree distributions.

Network	p_1	x_1	p_2	x_2	p_3	x_3	p_4	x_4
PNAS	0.950	3	0.538	3	0.453	13	0.077	347
PRE	0.240	5	0.931	3	0.253	5	0.129	91
PNAS-s	0.107	5	0.975	3	0.656	14	0.112	1,476
PRE-s	0.166	14	0.320	3	0.104	5	0.077	174
Synthetic-1	0.251	27	0.087	11	0.081	10	0.108	371
Synthetic-2	0.111	17	0.368	6	0.346	6	0.077	81

Indexes p_1 and p_2 are the p -values of KS test, measuring the goodness of fitting the heads of degree and hyperdegree distributions by generalized Poisson distributions. Indexes x_1 and x_2 are the right bounds of the corresponding fitting distributions. Indexes p_3 and p_3 measure the goodness of fitting the tails by power law functions with an exponential cutoff. The values of x_3 and x_4 are the left bounds of the corresponding fitting functions.

Table 7. Boundary point detection algorithm for $C(k)$ and $N(k)$ [21].

Input: Data vector $h_0(s), s = 1, \dots, K$, rescaling function $g(\cdot)$, and fitting model $h(\cdot)$.

For k from 1 to K do:
 Fit $h(\cdot)$ to $h_0(s), s = 1, \dots, k$ by regression;
 Do KS test for two data vectors $g(h(s))$ and $g(h_0(s)), s = 1, \dots, k$ with the null hypothesis they coming from the same continuous distribution;
 Break if the test rejects the null hypothesis at significance level 5%.

Output: The current k as the boundary point.
